Precipitation-driven typology of storms in the Alps

Georgia Papacharalampous[1,*], Eleonora Dallan[1], Moshe Armon[2], Joydeb Saha[1,3], Colin Price[4], Marco Borga[1], and Francesco Marra[5]

[1] Department of Land, Environment, Agriculture and Forestry, University of Padova, Legnaro, Italy

[2] The Fredy and Nadine Herrmann Institute of Earth Sciences, The Hebrew University of Jerusalem, Jerusalem, Israel

[3] National Centre for Medium Range Weather Forecasting, Noida, India

[4] Porter School of the Environment and Earth Sciences, Tel Aviv University, Tel Aviv, Israel

[5] Department of Geosciences, University of Padova, Padova, Italy

[*] Correspondence: georgia.papacharalampous@unipd.it, papacharalampous.georgia@gmail.com

Precipitation-driven typology of storms in the Alps

Georgia Papacharalampous[1,*], Eleonora Dallan[1], Moshe Armon[2], Joydeb Saha[1,3], Colin Price[4], Marco Borga[1], and Francesco Marra[5]

[1] Department of Land, Environment, Agriculture and Forestry, University of Padova, Legnaro, Italy

[2] The Fredy and Nadine Herrmann Institute of Earth Sciences, The Hebrew University of Jerusalem, Jerusalem, Israel

[3] National Centre for Medium Range Weather Forecasting, Noida, India

[4] Porter School of the Environment and Earth Sciences, Tel Aviv University, Tel Aviv, Israel

[5] Department of Geosciences, University of Padova, Padova, Italy

[*] Correspondence: georgia.papacharalampous@unipd.it, papacharalampous.georgia@gmail.com

Abstract: Numerous advances in precipitation science hinge on our ability to categorize storms into homogeneous classes, for instance to isolate time series with convective- or stratiform-like characteristics. Nonetheless, achieving such classifications remains challenging. Here, we use an Alpine storm typology developed through a straightforward methodology for unsupervised classification based on gauge-based precipitation only. From a vast sub-hourly dataset, we extracted over 790,000 independent storm time series. To categorize these, we employed a resampling-based partitioning algorithm, optimal in clustering big data. The algorithm revealed five dominant storm classes, with distinct characteristics in terms of maximum sub-hourly intensity, total storm volume, total duration and temporal variability, and clear spatial organization. Examination of additional characteristics (month of initiation, solar time at maximum intensity and lightning count) prompts us to suggest one class is likely associated with convective-like events (high intensities, peaks in summer and afternoon, strong association with lightning) and one is likely associated with stratiform-like events (medium intensities, large volumes, long durations, low association with lightning). A third class is characterized by moderate intensities and volumes, and relatively short durations, while the remaining two classes gather minor storms. The proposed typology could support modelling applications, such as class-specific stochastic simulation, class-informed bias adjustment of climate projections or multi-class extreme value analyses. Investigations of its climatological traits revealed, among others, higher activity of the convective-like class in recent years and specific Alpine regions. We provide the historical occurrences of the classes as an open dataset to facilitate further investigation of Alpine storm dynamics.

Keywords: convective-like precipitation; storm climatology; storm time series clustering; stratiform-like precipitation; sub-hourly precipitation; precipitation trends

1. Introduction

Analyzing precipitation storm time series and their climatology is crucial for mitigating hazards such as floods, landslides and debris flows, and adapting to changing climatic conditions (D'Odorico et al. 2005; Merz et al. 2014; Breugem et al. 2020; Kahraman et al. 2021). A specialized branch of such analyses is devoted to the separation of storms into homogeneous classes, similar to how floods and other hydrological events are commonly categorized (e.g., Hirschboeck 1988; Merz and Blöschl 2003; Turkington et al. 2016; Oppel and Fischer 2020), with the focus here being on the differentiation between convective-like and other events (e.g., Tremblay 2005; Ruiz-Leo et al. 2013; Feloni et al. 2019; Sottile et al. 2021; Dallan et al. 2022; Araujo et al. 2023; Treppiedi et al. 2023; Laaha et al. 2025). Beyond its role in advancing our comprehension of precipitation processes, this separation has numerous direct implications for stochastic modelling, extreme value analysis, and model uncertainty reduction (Blöschl et al. 2019; Fischer et al. 2019; Fischer and Schumann 2021; Marra et al. 2021; Sottile et al. 2021).

Indeed, the distinct mechanisms driving storm generation in each class may necessitate tailored weather generators (e.g., Kaczmarska et al. 2014; Peleg and Morin 2014; Tseng et al. 2025; Laaha et al. 2025) and operational weather forecasting models (e.g., Papadopoulos et al. 2005; Gustafsson et al. 2018; Zhou et al. 2019), or class-specific bias correction methods for climate model simulations (Maraun et al. 2017). At the same time, deriving physically meaningful typologies is challenging, if at all possible. This is due to the high complexity of the storm generation process, which involves interactions of a variety of physical mechanisms across a wide range of temporal and spatial scales (Grazzini et al. 2019), and the absence of physical information on the relevant physical variables at the scales of interest (e.g., vertical lifting velocities at hundreds of meters of scale). This challenge is even more difficult, but often necessary to tackle, by using only precipitation data from gauges. For this particular setting, which is also the focus of this study, thresholds on the maximum precipitation intensity or the decorrelation time have been defined to separate storms into types (e.g., Dallan et al. 2022; Araujo et al. 2023). However, these thresholds carry a strong degree of subjectivity and, consequently, ongoing efforts are devoted to their replacement with more objective methodological means, including curve clustering (e.g., Sottile et al. 2021; Treppiedi et al. 2023) and feature-based clustering (e.g., Grazzini et al. 2019; Laaha et al. 2025) from the algorithmic family of unsupervised machine learning (Hastie et al. 2009, ch. 14; James et al. 2013, ch. 10).

A general storm typology for the Alpine range (Section 2.1), a geographically complex territory attracting major interest in the study of precipitation dynamics (e.g., Frei and Schär 1998; Weisse and Bois 2001; Isotta et al. 2014; Ménégoz et al. 2020; Napoli et al. 2023; Estermann et al. 2025) and their links to hydrological extremes (e.g., Blanchet et al. 2025), is still lacking. The closest available storm typology was proposed by Grazzini et al. (2019), but it covers only extreme (heavy) precipitation events in Northern Italy and requires information on several atmospheric variables, in addition to precipitation time series. The data are also not openly available, which prevents their use in broader modelling contexts. Likewise, Laaha et al. (2025) developed a storm typology for a single location in Austria, relying on a combination of precipitation and lightning features. Neither study was accompanied by extended analyses of the climatological traits of the storm classes. A particularly urgent need, in this regard, is the detection of trends in the occurrence rates of the various classes (e.g., Rulfová and Kyselý 2014; Llasat et al. 2021; Treppiedi et al. 2023), which may provide direct hints on the expected impacts of the ongoing climate change.

In light of the current gaps in our understanding of the Alpine storm patterns, a clustering analysis relying solely on precipitation measurements from gauges (as done for other regions, e.g., by Sottile et al. (2021) and Treppiedi et al. (2023)) may offer several key advantages. First, it could ensure reasonably broad applicability across diverse geographical settings, particularly since supplementary datasets (such as radar or reanalysis) have limited availability across many locations and may be subject to diverse processing methodologies. Second, it could enable a more precise identification of localized rainfall patterns, thereby preventing the misattribution of broad weather system characteristics to specific localized precipitation behaviors, an important risk for clustering approaches based on atmospheric variables, such as those by Grazzini et al. (2019) or Flaounas et al. (2023).

Given the state-of-the-art and the rationale outlined above, our study provides a new, versatile and reproducible means of deriving precipitation-driven storm typologies, designed to have reduced subjectivity compared to the threshold-based methods. It also provides the first storm clustering method capable of extracting information from big, high-resolution precipitation datasets, which is crucial for drawing as much of the available information as possible in general, and particularly for the case of the Alps. Additionally, the study introduces the first openly available storm typology for the Alpine region, which will serve as a foundation for future climatological and hydrological applications. Specifically, our aims were to:

1) Develop a framework for deriving storm typologies from precipitation datasets of any size, and particularly from big datasets. Simplicity and versatility were also deemed important, as they may allow transferability around the globe after marginal adjustments based on the regional climatology or local interests.
2) Introduce an objectively-derived, precipitation-driven typology of Alpine storms, leveraging a big precipitation dataset. This typology should comprise storm classes with distinct characteristics that reflect domain knowledge.
3) Investigate the unexplored climatology of the Alpine storm classes in the extensive dataset by addressing the following key questions:
   a) How does the proportion of the classes vary in space?
   b) How do the seasonal occurrence rates of the classes vary in space?
   c) Has the relative proportion of the storm classes changed over time?

2. Study area and data

2.1 Study area

We studied storms that have occurred in and around the Alps (Figure 1), a region with a wide range of climates — mainly alpine (polar), boreal (snow) and warm temperate, according to the updated Köppen-Geiger classification by Beck et al. (2018). Largely due to the strong influence of mountainous topography on local precipitation especially near the sea (Buzzi et al. 1998), the Alps offer a compelling setting for the study of precipitation storm patterns and their climatology (Rubel et al. 2017). Compared to other regions, the Alps exhibit a higher proportion of high-intensity wet days (Isotta et al. 2014), a larger proneness to extreme storms (Grazzini et al. 2019) and higher lightning counts (Kahraman et al. 2022). The precipitation climatology of the greater Alpine region has been analyzed, for instance, by Frei and Schär (1998), Isotta et al. (2014), Ménégoz et al. (2020) and Napoli et al. (2023). The mean annual precipitation is typically higher than the surrounding floodplains due to orographic enhancement, reaching values as high as 3000 mm year^{-1}. The central region receives lower precipitation amounts, on the order of 900 mm year^{-1}, due to the protection effect played by the surrounding mountains (Borga et al. 2005).

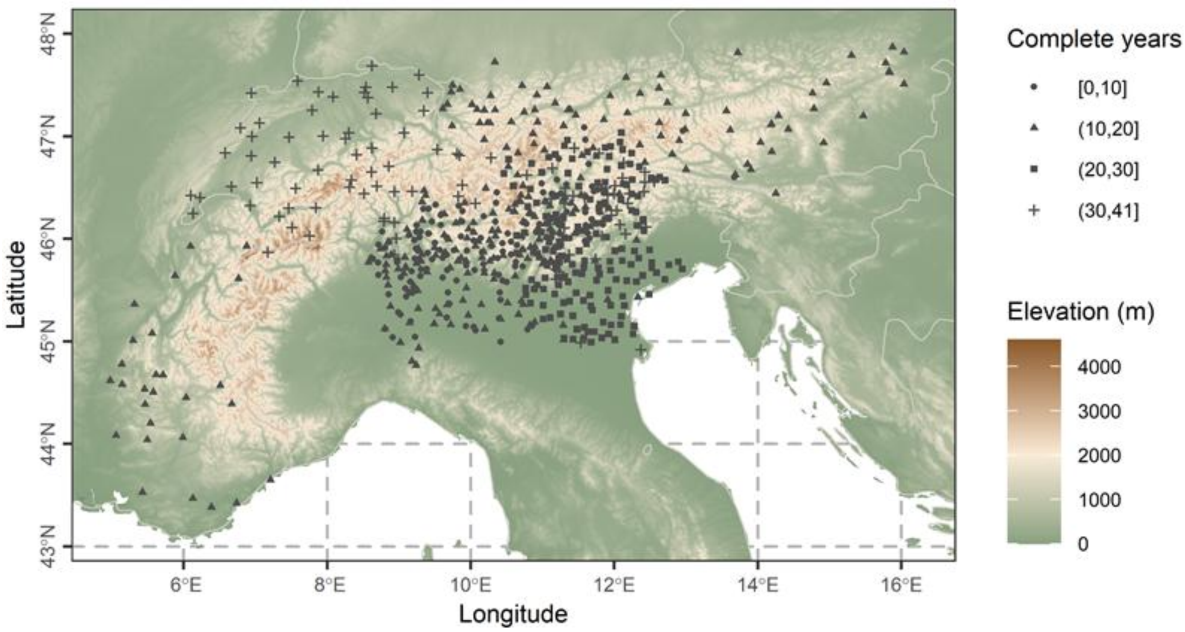

Figure 1. Study area, its topography (extracted from the Amazon Web Services Terrain Tiles), geographical locations of the precipitation stations and number of complete years of available data for each of these stations.

2.2 Precipitation data

We compiled a comprehensive dataset of sub-hourly precipitation measurements from seven data sources (Appendix A) and 670 instrumental stations across five countries (Figure 1): Italy (505 stations), Austria (74 stations), Switzerland (61 stations), France (27 stations), and Germany (3 stations). Based on the Amazon Web Services Terrain Tiles (https://registry.opendata.aws/terrain-tiles), the elevations at the locations of the stations range between −4 and 3,214 m, with a mean and a standard deviation approximately equal to 773 and 627 m, respectively. Subsets of our dataset were previously used in the studies by Dallan et al. (2023, 2024), Marra et al. (2024), Correa-Sánchez et al. (2025) and Peleg et al. (2025), which addressed different research questions.

From the original sources, we extracted time series of varying temporal resolutions (5-, 6- and 10-min), which we then homogenized through time series aggregation to the 10- or 12-min temporal resolution, with the latter being the case for the time series from France. Additionally, time zone homogenization was conducted and quality issues (i.e., missing values/dates, negative and other unrealistic values, duplicate dates) were identified and treated. Time series data records corresponding to calendar years with more than 10% of their values missing were excluded from our final dataset. This dataset comprises complete sub-hourly precipitation time series with varying lengths, observed during the course of 44 years (1981–2024). From these time series, we subsequently extracted the precipitation storm time series, as detailed in Section 3.1. The number of complete calendar years per location is summarized in Figure 1. Data for at least 30 complete calendar years are available for 113 locations, allowing for trend analyses (Section 3.5).

2.3 Lightning count data

There is a well-known association between convective precipitation and lightning occurrence (Soriano et al. 2001; Papadopoulos et al. 2005; Pineda et al. 2007). Consequently, lightning counts can be used to independently investigate distinctions between convective-like and other storm time series (Feloni et al. 2019). Such data, and more precisely cloud-to-ground lightning counts derived from the World Wide Lightning Location Network (WWLLN; https://wwlln.net), are available for a large and representative portion of the stations and storms we examined. Herein, we exploited them in our post-clustering investigations (Section 3.4). Detailed information about the WWLLN network can be found in Rodger et al. (2006) and Virts et al. (2013). Given that the storms often spanned multiple days, the maximum daily lightning count was extracted for each storm. To ensure consistency and account for uncertainty in the geolocation, lightning strikes were counted within a ±0.5° grid box centered on the location of each station. Temporal alignment was achieved by matching the WWLLN lightning data to the storm time ranges.

3. Methods

3.1 Storm time series extraction

Precipitation storm time series, representing wet periods that are independent in time, were extracted from the merged precipitation dataset (Section 2.2) following the methodology described in Marra et al. (2020). Considering the climatology of the Alps, independence was ensured by imposing the lower threshold of 24 hours in the length of the dry spells between storms. Storms with a duration of at least 30 min were included in our precipitation storm database.

3.2 Storm clustering

To classify the precipitation storm time series, we formulated a methodology employing unsupervised machine learning. This approach is increasingly used for developing storm typologies (e.g., Grazzini et al. 2019; Sottile et al. 2021; Laaha et al. 2025) and, more generally, event typologies in the field of hydrology (e.g., Markonis et al. 2021; Fischer and Schumann 2024), owing to its objectivity and scalability, qualities that align well with the objectives of this study. Our clustering methodology is feature-based, aiming at maximizing intra-cluster homogeneity and inter-cluster heterogeneity based on the following four diverse features extracted from the precipitation storm time series (Section 3.1): (a) maximum (peak) intensity, (b) total volume, (c) total duration, and (d) coefficient of variation. The first three, in particular, are established as key features in the study of storms (e.g., Herrera et al. 2023), while the coefficient of variation is a standard feature in stochastic analysis that can also be used to quantify gradients of variability. To maintain simplicity and avoid redundancy, we did not employ more features for the clustering.

To address scalability challenges (specifically, the large RAM storage requirements) posed by our large dataset (Section 2.2), which could not be handled by conventional non-hierarchical clustering algorithms (e.g., the well-known k-means and k-medoids described in detail in Hastie et al. 2009, ch. 14.3.6 and 14.3.10), we selected CLARA (Clustering Large Applications; Kaufman and Rousseeuw 1990, ch. 3) as the core algorithm. In summary, CLARA is a resampling-based partitioning algorithm (Hopke and Kaufman 1990) applying k-medoids. These exhibit larger robustness to noise and outliers with respect to k-means, as they use actual data points (the “medoids”) as cluster centers instead of computing their cluster centers (the "centroids"). Within CLARA's framework, the k-medoids are applied to cluster a random sample of the data, with this process being repeated multiple times. The best clustering solution is then selected based on a minimum dissimilarity distance measure and finally applied to the entire dataset. In this study, the sample number and sample size were set to 10,000 and 1,000, respectively. The dissimilarities were calculated using Euclidean distances.

To ensure that CLARA would not be affected by skewness and different scales in the features, feature preprocessing took place. More precisely, the feature values were first transformed and then standardized. Log-transformation was applied to the maximum intensity, total volume and total duration, and square-root transformation was applied to the coefficient of variation (due to the existence of zeros in the values of this latter feature). Standardization of the storm duration and coefficient of variation took place for all the stations together, while it was done for each station separately, for the maximum intensity and total volume. This distinction was made because the latter two features are expected to strongly depend on local climatological conditions, in contrast to the former two (e.g., Avanzi et al. 2015).

3.3 Storm-level characteristics of the classes

The storm classes, obtained through clustering, were initially explored with the four defining features (Section 3.2) and through visual inspection of the storm-type-labelled precipitation storm time series. We then investigated the classes based on three storm-level features that were not involved in the clustering: seasonality (month at the storm initiation), diurnal cycle (solar time at the first occurrence of the maximum intensity — note that the maximum intensity may appear more than once in storm time series, especially for sub-hourly temporal resolutions) and lightning count. The month at the storm initiation was extracted from the storm time series (Section 3.1). The solar time at the (first) occurrence of the maximum intensity was chosen over the local time to better reflect the sun's position in the sky and its influence on storm dynamics. It was estimated based on the respective UTC time (which was extracted from the storm time series; Section 3.1) and the longitude at the location of the storm. Lightning count validation was performed on a reduced but still large sample, due to limitations in the availability of lightning data (Section 2.3).

3.4 Spatial organization of the classes and key events

To ensure that the classes, identified from local time series, are meaningful, it is important to verify their spatial consistency. We therefore computed the occurrence rate of each storm class in the neighborhood of each given class on the same day. More precisely, we examined each storm in each station, inspecting the occurrence of the storm class itself as well as the occurrences of the remaining storm classes in distance intervals of: (0, 10], (10, 20], (20, 50], (50, 100], (100, 200], and (200, 500] km. We only included storms in this computation, meaning that dry stations in the examined neighborhood were not considered.

Additionally, we examined the spatial pattern of storm states across the Alpine range for eight case studies. These included three random dates in the winter and early spring (2006-03-10, 2012-01-08, 2013-01-27), as well as five dates when events that are well-known to the research community occurred in the region of interest, such as the Vaia storm (2018-10-29; Davolio et al. 2020), the Lausanne flood (2018-06-11; Gabella et al. 2019), the Vizze flood (2012-08-04; Destro et al. 2018), the Magra flood (2011-10-25; Amponsah et al. 2016), and the Lierza flood (2014-08-02; Borga et al. 2019). These selected benchmark events have been comprehensively documented and characterized in the literature as either "convective" or "stratiform" drawing on radar investigations, thereby providing a reliable reference for capturing possible linkages to precipitation processes.

3.5 Storm type climatology analysis

We performed a climatology analysis of the storm classes based on three independent parts. In the first, we computed the aggregate occurrence rates of each class at each geographical location (all years and seasons combined). In the second, we computed seasonal (DJF, MAM, JJA, SON) occurrences within each class at each geographical location. To make the identification of spatial patterns easier, the occurrence rates (%) from the first two parts were grouped into the following categories: [0, 10], (10, 20], (20, 30], (30, 40], (40, 50], (50, 60], (60, 70], (70, 80], (80, 90], and (90, 100]. Then, we analyzed the climatology variations in time, following two steps: (a) computation of the occurrence rates of the classes within each of the consecutive time periods 1981-1990, 1991-2000, 2001-2010, and 2011-2023; and (b) trend analysis for 113 stations with at least 30 complete years of precipitation data (Figure 1). The latter comprised the computation of the slope of the linear regression line and performance of the Man-Kendall trend test (Mann 1945; Kendall 1975), with the null hypothesis being correlation zero (no monotonic trend) and p-values smaller or equal to 0.05 suggesting strong evidence against the null hypothesis and, thus, trend. Both (a) and (b) were conducted for three different settings: all seasons combined; summer only (JJA); and the remaining seasons (DJF, MAM and SON).

4. Results and discussion

4.1 Precipitation storm database

Our precipitation dataset yielded a collection of 792,786 storm time series of varying sizes and characteristics (Appendix A). The size of this collection surpasses that of the largest existing precipitation storm collections (e.g., Herrera et al. 2023), as well as that of other remarkably large event datasets in the field (e.g., Stein et al. 2020; Tarasova et al. 2020). Combined with its fine (sub-hourly) temporal resolution, this dataset provides a robust basis for our storm typology.

4.2 Analyzing storm types through their driving features

The division into five classes led to domain-interpretable patterns based on the features driving the clustering (Figure 2), consistent with our aim to derive a storm typology that satisfactorily reflects precipitation in the Alps. The key role of domain knowledge in validating clusters towards achieving optimal clustering solutions is emphasized in the statistical learning literature (James et al. 2013, ch. 10.3). Indeed, divisions into fewer classes did not allow homogeneous classes to discernibly emerge, while divisions into more classes led to outcomes without clear domain meaning. For instance, a six-cluster division yielded a similar structure, with one of our five clusters being subdivided into two without a clear added value from a domain-interpretability perspective.

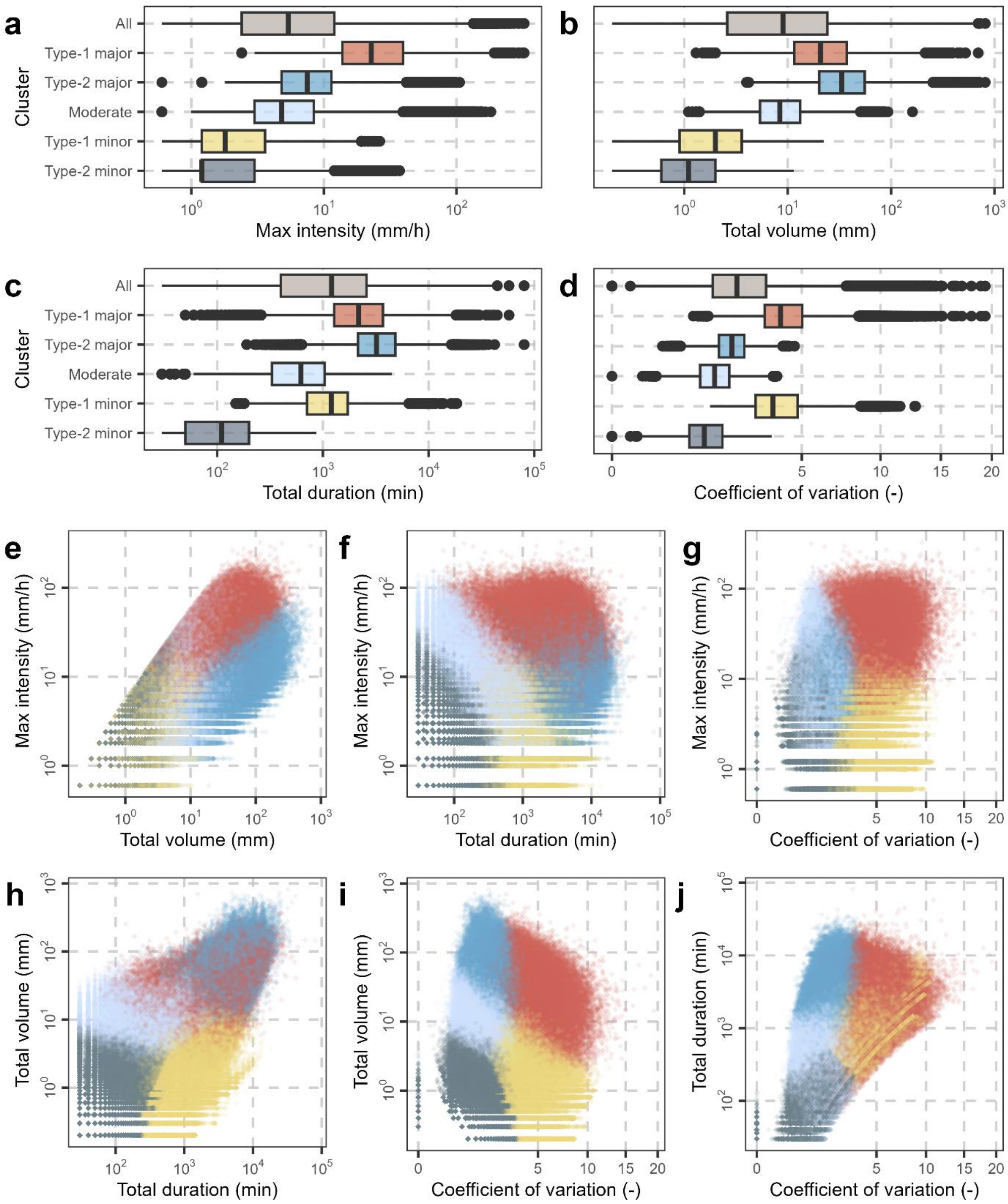

Figure 2. Analysis of the (a) maximum intensity, (b) total volume, (c) total duration and (d) coefficient of variation values characterizing the clusters, and (e-j) investigations of the relationships between these values.

Overall, a five-class typology seems reasonable. We expected at least two important classes to emerge, one broadly related to storms with high maximum intensities and relatively high total volumes ("type-1 major"), and another associated with storms with long total duration and high total volumes ("type-2 major"). Additionally, we anticipated one or more classes capturing less significant phenomena or events that our gauge-based time series cannot fully resolve, given the coarse spatial coverage and fine temporal resolution of the rain gauges ("minor" classes). These expectations align with previous storm classification studies. For instance, Rulfová and Kyselý (2013) and Cipolla et al. (2020) included classes comprising "mixed" and "unresolved" events. Similarly, Sottile et al. (2022) identified four clusters of 10-min precipitation storm time series observed in Sicily, Italy: two of "convective" nature, one of "possibly convective" nature, and one of "stratiform" nature. Lastly, our expectations are also consistent with Grazzini et al. (2020), who considered three classes of "frontal", "intermediate" and "deep convective" origins while classifying only the extreme storm events in the Alps.

The overall characteristics of the classes that emerged from our analysis are as follows. The "type-1 major" class (156,295 storms) comprises the storms with the highest maximum intensities (Figure 2a), among the highest total volumes (Figure 2b) and the highest coefficient of variation values (Figure 2d). Storms belonging to the "type-2 major" class (182,309 storms) have medium maximum intensities (Figure 2a), the highest total volumes (Figure 2b), the longest total durations (Figure 2c) and low coefficient of variation values (Figure 2d). The "moderate class" (190,385 storms) is characterized by maximum intensities and coefficients of variation of similar magnitude as the "type-2 major" class (Figure 2a, d), though its total volumes are somewhat smaller (Figure 2b) and its total duration is much shorter (Figure 2c). Lastly, the "type-1 minor" (136,056 storms) and "type-2 minor" (127,741 storms) classes have mostly low maximum intensities (Figure 2a) and mostly low total volumes (Figure 2b). The latter contains all the minor storms with short total durations and low coefficient of variations, and the "type-1 minor" those with medium total durations and high coefficient of variations (Figure 2c, d). Visual examination reveals that the "type-1 minor" class comprises storm time series resembling those of the "type-2 minor" class but punctuated by relatively long dry periods. The "type-1 minor" and "type-2 minor" classes likely reflect intermittent station exposure to storm events, a fact further highlighting the challenges in establishing a fully definitive and physically consistent (or even fully domain-interpretable) typology from point measurements.

It is important to note that our storm classes demonstrate robustness to data perturbations. Indeed, subsampling experiments that included the removal of entire regions (results not presented here for reasons of brevity) consistently produced classes with similar features. This robustness is a notable advantage, as many clustering methods are sensitive to such perturbations (James et al. 2013, ch. 10.3.3). Furthermore, in their review of flood classifications, which offers insights that are also applicable to storm classifications, Tarasova et al. (2019) identify robustness (which they define as the ability to obtain similar classes using different data sources) as a critical characteristic for event typologies. In addition, while the exact form of our storm types may not be globally transferable, our clustering methodology is, due to its simplicity and versatility. Consequently, our overall framework also aligns with the transferability and adaptability requirements emphasized in the same review.

4.3 Additional storm-level features by class

Investigation of storm-level features that were not used for the clustering (Figure 3) allows us to explore additional important, and potentially physically suggestive, aspects of every class that were deliberately omitted from the method to keep it simple. The "type-1 major" class peaks during summer (Figure 3a) and in the afternoon (Figure 3b), and is associated with frequent lightning activity (Figure 3c). In contrast, the "type-2 major" class shows a bimodal distribution with peaks in spring and autumn (Figure 3a), an almost flat distribution in its diurnal cycle (Figure 3b) and relatively low lightning activity (Figure 3c). The remaining classes exhibit relatively flat distributions across seasons and diurnal cycles, and are characterized by negligible lightning activity.

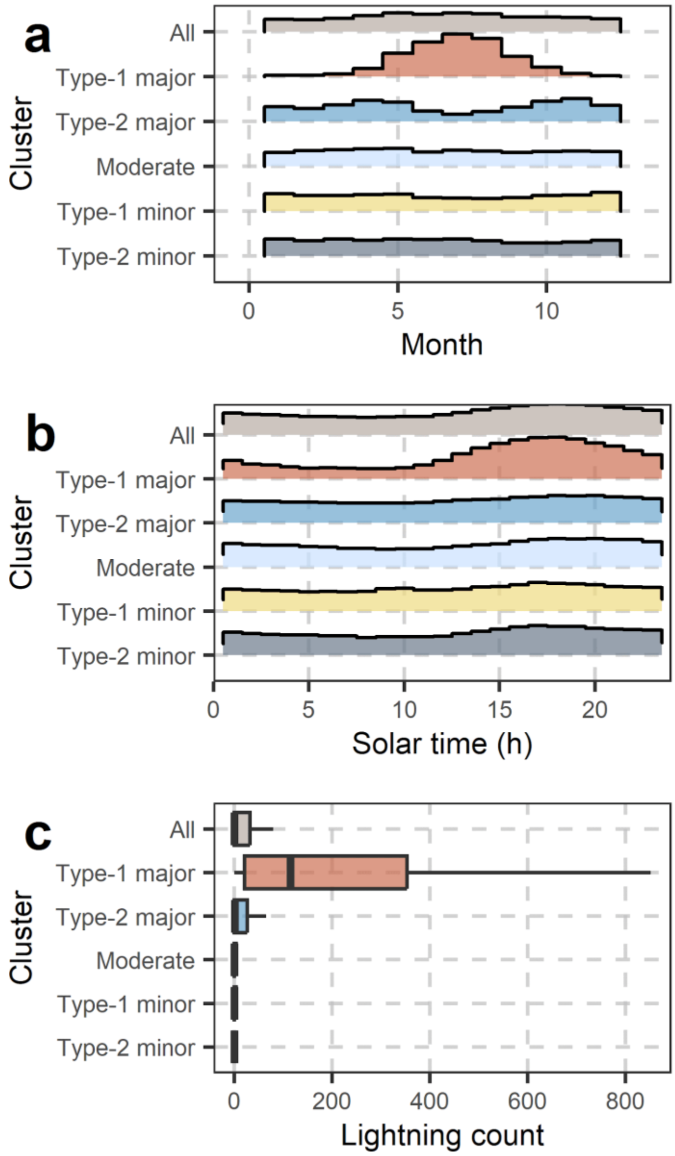

Figure 3. Analysis of the clusters with respect to their: (a) seasonality; (b) solar time at the (first) occurrence of the maximum intensity; and (c) lightning counts (outliers have been removed for clarity).

4.4 Spatial organisation of the classes and key events

Spatial organisation characterizes the historical occurrences of all storm classes, with each of them having occurred far more frequently in the vicinity of its own events on the same day than any other class, at least for distances up to 50 km (Figure 4; see the side-by-side boxplots on the main diagonal thereon). The "type-2 major" class exhibits the largest degree of spatial clustering. Its historical occurrence rates exhibit a median equal to about 75% for distances smaller than 10 km, meaning that storms observed within 10 km from a "type-2 major" storm are classified as the same type about 75% of the time. This median gradually decreases to about 50% for distances of 200 to 500 km from the analyzed storm. The “type-1 major” class exhibits the second largest degree of spatial clustering, with median occurrence rates around 65% at distances smaller than 10 km, decreasing to still more than 30% at 200–500 km distances. With the respective occurrence rates being found equal to about 55% and larger than 15%, the “moderate” class exhibits the third largest degree of spatial clustering and graduality in the reduction of these rates with the distance. From a different angle, the distances at which the median rates are closest to 50% are 100, 200 and 20 km for the “type-1 major”, “type-2 major” and “moderate” classes, respectively.

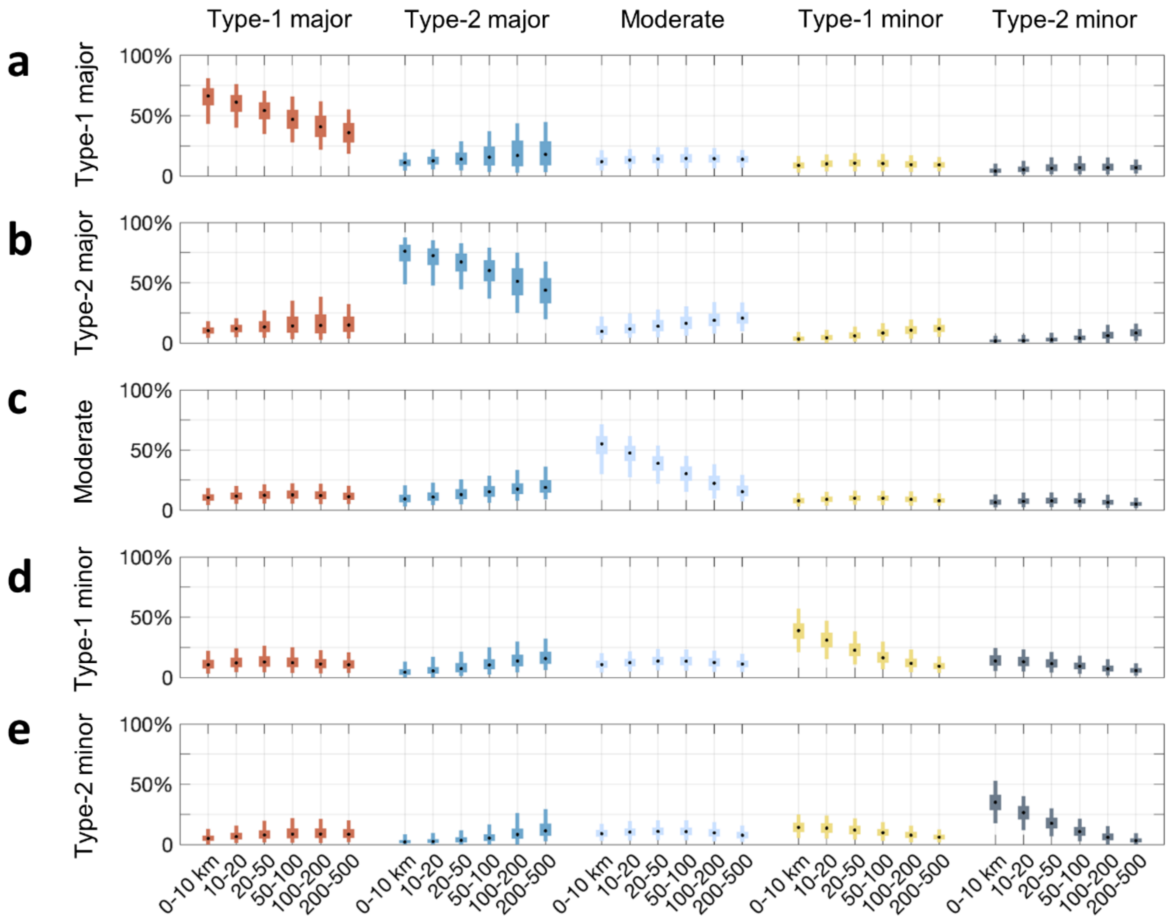

Figure 4. Occurrence rates of the classes in the wet stations within various ranges of distances from the (a) “type-1 major”, (b) “type-2 major”, (c) "moderate”, (d) “type-1 minor” and (e) “type-2 minor” classes.

For the “type-1 minor” and “type-2 minor” classes, the reduction in the occurrence rates with distance is more abrupt. This aligns with our expectations, as these classes are anticipated to correspond to unimportant storms or phenomena that were not well-captured by our gauges. For example, we expect the stations that only capture the outermost portions of an important event to only see a minor amount of precipitation.

Indeed, the median of these rates starts from about 40% for distances less than 10 km and becomes less than 25% already for distances between 20 and 50 km. Moreover, as the distance from a storm observation increases, the occurrence rates of different classes increase notably for some pairs of classes, such as the {“type-2 major”, “type-1 major”} and {“type-2 major”, “moderate”}. For other pairs, they remain similar or tend to only slightly increase.

Figure 5 contributes to a more intuitive understanding and complete understanding of the classes. In winter and early spring (Figure 5a, c, e), the “type-2 major”, “moderate”, “type-1 minor” and “type-2 minor” storm classes display noticeable spatial clustering, with this clustering being more pronounced for the first two classes. In contrast, “type-1 major” storms during these seasons show no apparent spatial clustering and appear randomly distributed. On dates with high-impact storm events (Figure 5b, d, f-h), however, the “type-1 major” class also displayed strong spatial clustering, with their corresponding phenomena often covering large areas. Meanwhile, both “minor” classes occurred only sporadically, appearing randomly distributed, typically on the periphery of the wet region.

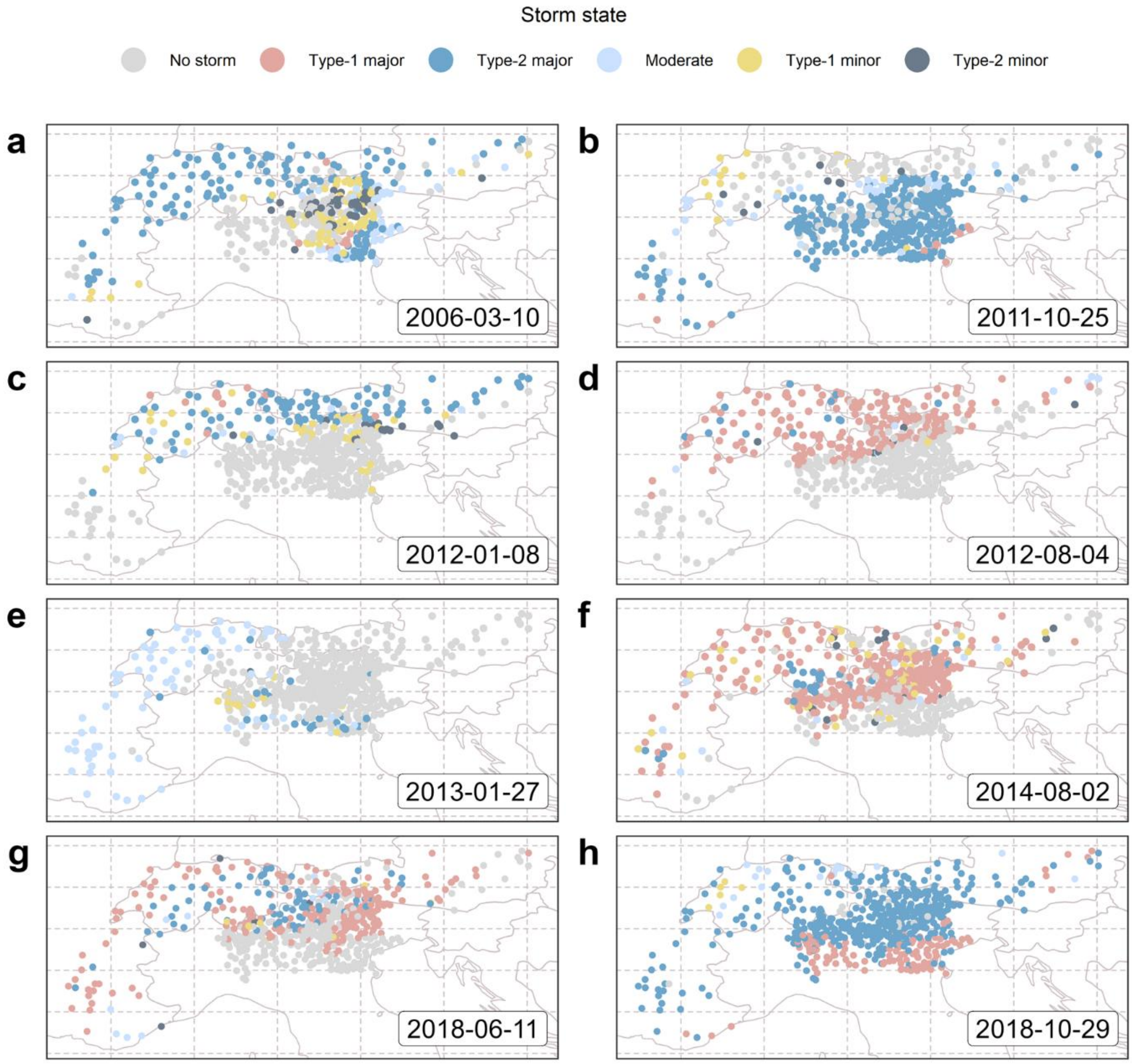

Figure 5. Storm state at stations with data on (a, c, e) random dates in the winter or early spring and (b, d, f-h) dates when well-known storm events occurred.

Notably, heavy rainstorms with large spatial extent were observed in northern Italy on October 25, 2011 (Amponsah et al. 2016), which our clustering method attributed to the "type-2 major" class (Figure 5b). Also notably, the storm that led to a severe flash flood and numerous debris flows in the Vizze valley (Eastern Italian Alps) on August 4, 2012 (Marra et al. 2014; Destro et al. 2018) was classified as "type-1 major" (Figure 5d). On August 2, 2014 (Figure 5f), high-intensity, short-duration rainfall caused the Lierza river (Eastern Italian prealps) to burst its banks, leading to severe flash flooding and landslides in Veneto, northern Italy (Borga et al. 2019). Our clustering method identified "type-1 major" storms in those areas on that date. Similarly, on the late evening of June 11, 2018 (Figure 5g), heavy thunderstorms and a record-breaking, high-intensity, short-duration storm caused flash flooding in Lausanne, Switzerland (Gabella et al. 2019). Our clustering method classified the storm occurrences near Lausanne on this date as "type-1 major". Finally, the Vaia storm that severely hit north-eastern Italy at the end of October, 2018 (Davolio et al. 2020), was identified as "type-2 major" with vast regions of "type-1 major" features, mostly in the southern lowlands (Figure 5h).

4.5 Storm type climatology

Figure 6 illustrates the historical proportions of the classes across the examined locations. Overall, "type-1 major" storms (Figure 6a) occurred at rates between 10% and 20% in many locations, including those in Switzerland and Germany, most of those in France and Austria, and about half of those in Italy. In the remaining locations, mostly including the largest part of Northeastern Italy, "type-1 major" storm occurrence ranged from 20% and 30%. The "type-2 major" storms (Figure 6b) were prevalent, occurring at rates from 20% to 30% in most Italian areas and some locations in France, Switzerland, Germany, and Austria. Higher occurrences, between 30% and 40%, were observed at almost all the remaining locations. Only a few lowland locations in Italy showed lower occurrences of this storm type. Rates of the "moderate" storms (Figure 6c) were more consistent across the various locations, with most experiencing occurrences between 20% and 30%. Small variations existed, with a few locations exhibiting rates slightly outside this range. Lastly, each of the minor classes (Figure 6d, e) generally represented 10% to 20% of the occurrences for most locations. However, the "type-1 minor" storms (Figure 6d) were more frequent (largely 20%-30%) for most of the examined lowland locations in Italy.

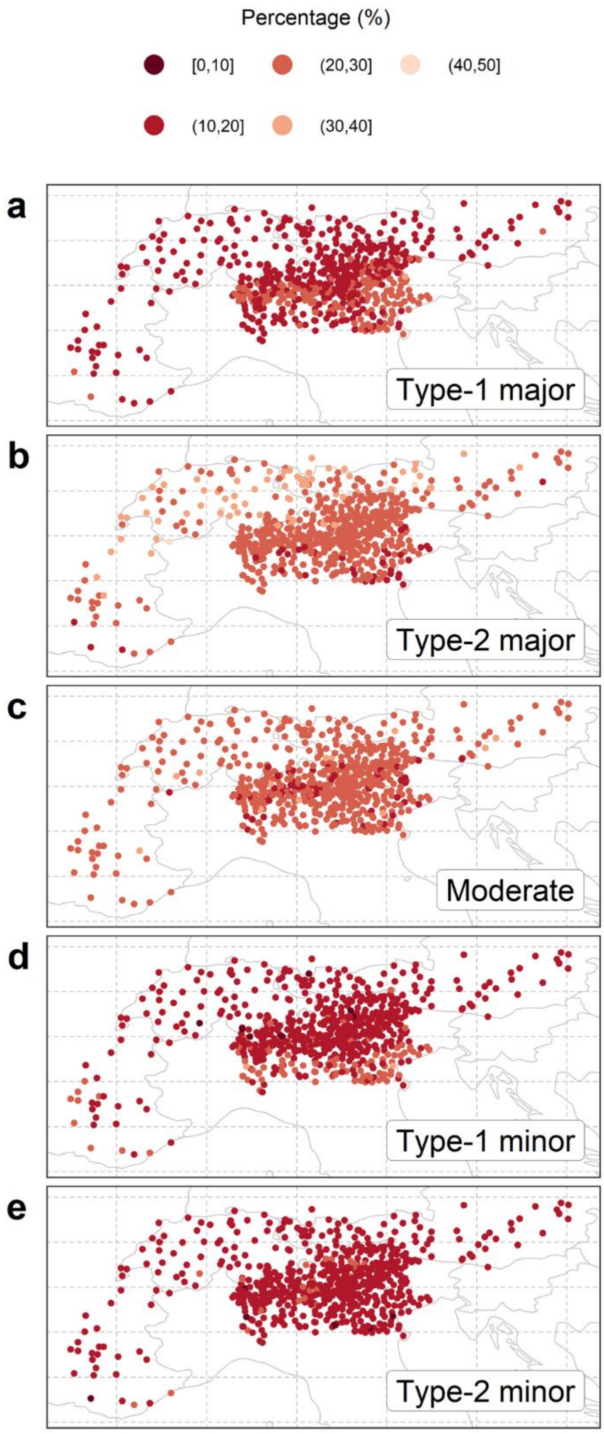

Figure 6. Proportions of the (a) “type-1 major”, (b) “type-2 major”, (c) “moderate”, (d) ”type-1 minor” and (e) “type-2 minor” classes in each geographical location.

Distinct spatial patterns characterize the historical occurrence rates of the “type-1 major” (Figure 7a, d, g, j) and “type-2 major” (Figure 7b, e, h, k) storm classes across the four seasons. For nearly all locations, the “type-1 major” class occurred at very low rates during winter (DJF), as also shown in Figure 3a, resulting in no notable spatial patterns for that season (Figure 7a). In contrast, “type-1 major” storms are most frequent in summer (JJA), and their occurrence rates (Figure 7g) reveal clear meteorological differences across regions, with rates increasing from south (40–50% at most locations) to north (50–80%) and from lowlands to highlands. In the spring (MAM) and autumn (SON), “type-1 major” storms appeared more often in low-elevation locations in Italy (rates 20–30% at most of them) than in the pre-Alps and Alps (rates below 20% at most locations). In the same seasons, the “type-2 major” storms showed high occurrence rates (40–50% at most locations), which however do not reveal clear spatial patterns. In the winter, they mostly occurred with lower rates for the pre-Alpine and Alpine areas in Italy (below 30%) than for other regions, while in the summer they occurred with low rates (below 10%) for the low-elevation locations in Italy and for southern locations in France and with somewhat larger rates (mostly 10–30%) for the remaining regions, likely reflecting a south-north gradient. Meanwhile, no notable spatial patterns were observed for the “moderate” storms across the four seasons (Figure 7c, f, i, l).

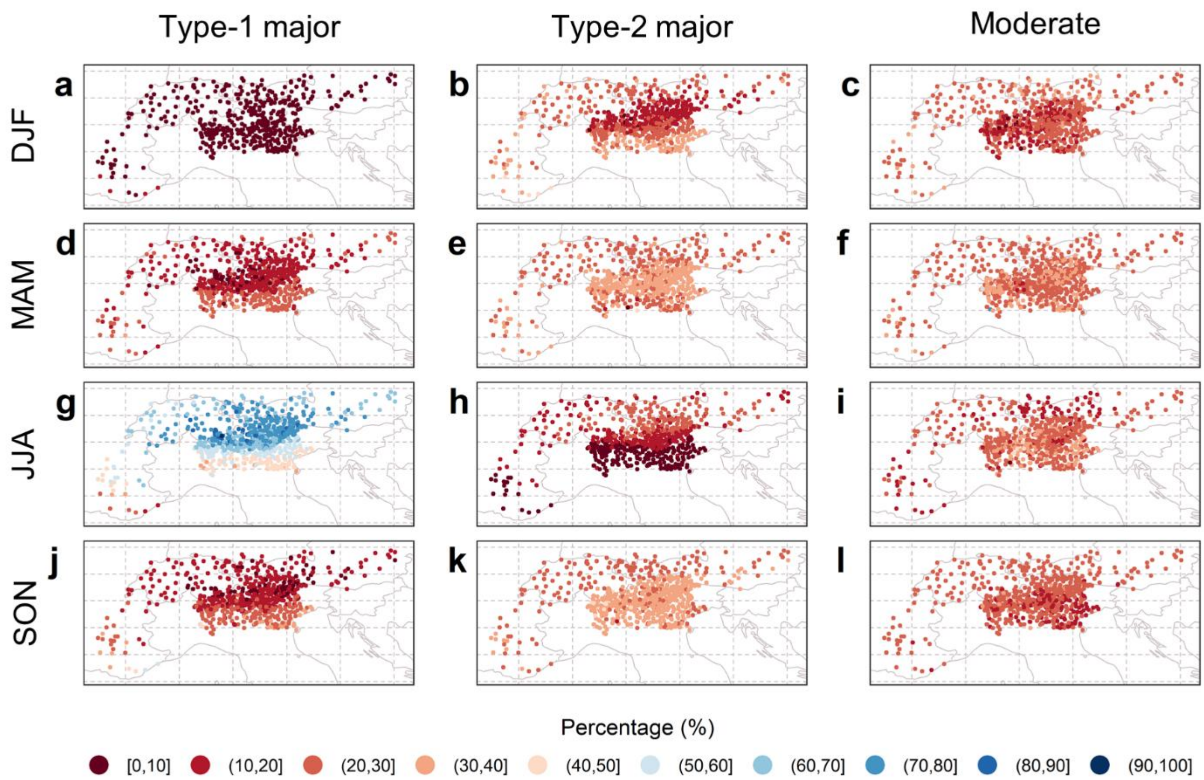

Figure 7. Proportions of the seasons within the (a, d, g, j) “type-1 major”, (b, e, h, k) “type-2 major” and (c, f, i, l) “moderate” classes.

Notable positive temporal changes were identified in the occurrence rates of the “type-1 major” class. Although noteworthy changes were observed across all seasons (Figure 8a, d), the summer changes (Figure 8b, e) were far more prevalent than those in the other seasons (Figure 8c, f). In particular, the trends were found to be statistically significant for about 22% and 27% of the stations offering long records for all the seasons (Figure 8d) and for summer (Figure 8e), respectively. At the same time, notable negative temporal changes were found for the occurrence rates of the “type-2 major” and “moderate” classes, especially for the summer season (Figure 8b, e), with statistically significant trends for about 16% and 19.5% of the stations, respectively.

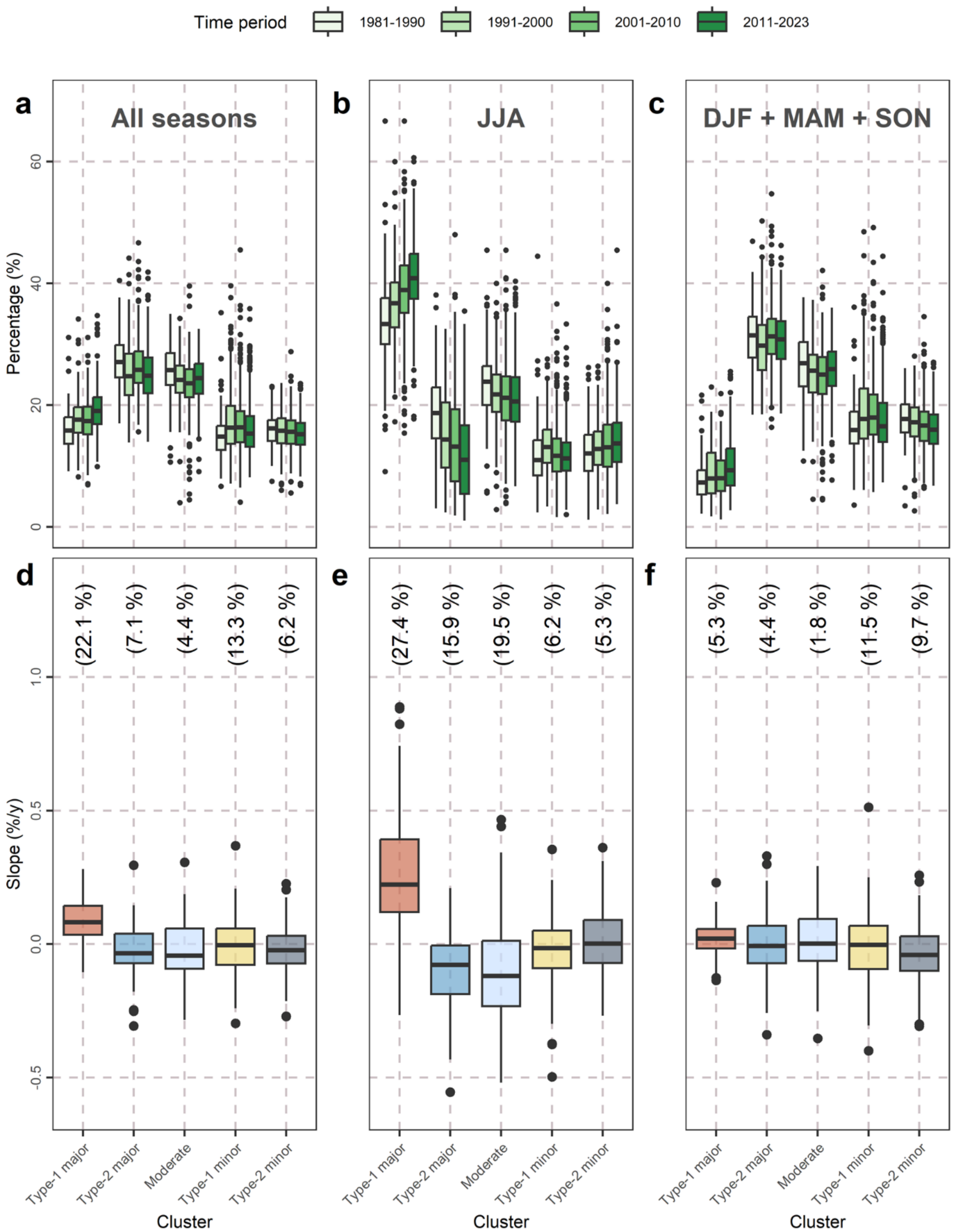

Figure 8. Analyses of the temporal changes in the occurrence rates of the classes at the various stations: (a-c) Percentages of the classes within consecutive time periods, and (d-f) trend analyses for the 113 stations with at least 30 complete years of precipitation data (see Figure 1), with the percentages of the stations with statistically significant trends reported at the top of the side-by-side boxplots of the linear slope estimates.

4.6 Possible association of the classes to precipitation processes

A synthesis of our findings (Sections 4.2-4.5) prompts us to suggest potential associations of the "type-1 major", "type-2 major" and "moderate" classes with distinct precipitation processes. The characteristics of the "type-1 major" storms (highest maximum intensities, summer and afternoon peaks, frequent lightning activity, summertime orographic uplift over the pre-Alpine and Alpine terrain) closely resemble those of convective events. Meanwhile, the "type-2 major" storms exhibit features typical of stratiform events: medium intensities, the highest total volumes, longest durations, bimodal spring/autumn peaks, low lightning activity and large spatial clustering. For the "moderate" class, we hypothesize that it may be associated with stratiform events where winds are orthogonal to the main cloud direction, resulting in properties similar to typical stratiform storms but with shorter total durations. No clear association can be made for the minor types, which may appear at the margins of large scale storms with no clear distinction between the two (see Figures 4 and 5), aside from the presence of a long dry period in the "type-1 minor" storms.

The potential linkages discussed above are further supported by consistency with independent characterizations of well-documented high-impact "convective" and "stratiform" events (see Section 4.4), including the Vaia, Vizze, Lausanne, Lierza and Magra storms (Amponsah et al. 2016; Destro et al. 2018; Borga et al. 2019; Gabella et al. 2019; Davolio et al. 2020). Moreover, Marra et al. (2026) provide further evidence for our interpretations of the two "major" types by demonstrating that most sub-hourly extremes belong to the "type-1 major" rather than "type-2 major" storms, while around 70% of the 24-hour extremes belong to the "type-2 major" storms (compared to 30% for "type-1 major"). Of course, it is important to emphasize that the interpretations offered here are not physically definitive, as our classification remains statistically based and data-driven. Establishing such physical linkages definitively would require different types of investigations, beyond the aims and contributions of this study and based on information that is not necessarily available at the scales of interest. Still, given the consistent and distinct features of each class across multiple dimensions, together with the alignment with independently documented benchmark events, our interpretations appear highly plausible.

When considering such potential linkages, it is essential to account for the station-based (or time series-based) nature of our clustering approach. For instance, the long total duration of the "type-1 major" class, which might initially appear inconsistent with typical convective event features, is better understood in light of our methodological context: our method classifies the entire storm time series (separated from previous and following storms by at least one dry day, and possibly comprising periods with diverse characteristics, including relatively long dry spells), not solely its “convective” component. Similarly, the large degree of spatial clustering observed for the same class, while seemingly at odds with intuitions about localized convection, becomes understandable when considering that individual convective cells are advected and can cover relatively large areas over the storm lifetime, and that the conditions favourable of generating convection may prevail over larger areas compared with the cell size, so there is a high chance of convection occurring at some point during the day over the area experiencing these conditions.

Building on the potential association of the "type-1 major" class with convective processes, the notable positive temporal changes identified in the occurrence rates of this class could be seen as aligning with findings by Dallan et al. (2022), who reported increasing trends in extreme short-duration precipitation in the north-eastern Italian Alps and attributed them to enhanced convective activity in summer. Our results may suggest that this signal extends beyond the area analyzed by these authors to the entire Alpine region, though further investigation would be needed to confirm this interpretation. Recent findings by Dallan et al. (2024), Estermann et al. (2025) and Peleg et al. (2025) further indicate that this increasing trend in heavy precipitation is expected to continue in the future, based on analyses of climate model projections.

5. Conclusion

This study introduces a precipitation-driven typology that separates the Alpine storms into five classes. This typology was informed by a collection of over 790,000 sub-hourly time series of independent storms extracted from a vast precipitation dataset spanning the Alpine range across five countries. A clustering method played a central role in the development of our proposed typology. This method objectively draws information from four key storm features estimated using precipitation time series: (a) maximum intensity, (b) total volume, (c) total duration, and (d) coefficient of variation. It was designed for simplicity and versatility to enable adaptations to diverse regions around the globe through marginal adjustments reflecting region-specific climatological characteristics. For the Alpine region specifically, the robustness of the clustering method in its current configuration was confirmed through its application to subsets of our storm collection. Because of its known optimality in clustering big data, a resampling-based partitioning algorithm was employed herein. However, conventional partition-based clustering algorithms, such as the k-means or k-medoids, are expected to exhibit similar efficiency in the absence of scalability issues.

Five distinct Alpine storm classes emerged from the clustering based on the four driving features. We also investigated three additional storm-level features not used in the clustering, specifically the month of the storm initiation, solar time at the (first) occurrence of the maximum intensity and lightning count corresponding to the storm. We further examined the extent to which the occurrences of each class were clustered in space and compared our labels for well-known, large-impact storms with findings from previous radar-based studies. Based on the consistency observed with known features of different storm types and with existing characterizations of the large-impact events, the proposed typology may serve various applications within the Alpine region. These could range from the development of stochastic simulation methods tailored to storm characteristics to the improvement of the bias correction for climate projections or to the advancement of process-based extreme value analyses. To support such efforts, we provide the historical occurrences of the classes alongside the storm features as an open dataset (Appendix A).

Fundamental questions in the study of storm typologies concern the climatology of the classes. Therefore, as a first application of the herein compiled storm typology, we performed a climatological analysis of its five types. We found the occurrence rates of the “type-1 major” storms, i.e., those with features potentially suggestive of convective processes, to vary with both location and season, and identified regions where the same rates were higher than in others for specific seasons, such as the lower-elevation regions in Italy during spring. We also found the same storms to be occurring with increasing frequency in more recent years, particularly during summer. These findings point to the potential of our proposed typology for understanding aspects of the Alpine precipitation dynamics and for serving as a useful framework for a variety of modelling purposes. This potential is additionally reflected in the straightforward integration of the typology into frameworks dedicated to extreme precipitation characterization and modelling in the Greater Alpine region (Dallan et al. 2025; Marra et al. 2026).

A direct validation of the storm classes against established large-scale weather types could provide insights into the linkage between storm-scale precipitation processes and prevailing atmospheric circulation patterns. However, such a one-to-one comparison is not trivial with currently available tools, as weather-type classifications describe atmospheric states on meso- to synoptic scales, thereby making it difficult to unambiguously associate individual storms from rain gauge time series with large-scale physical processes. Still, exploring this connection, even if only in a simplified form, could further enhance the interpretability and applicability of the proposed typology.

Acknowledgements: This study was carried out within the RETURN Extended Partnership, funded by the European Union Next-GenerationEU (National Recovery and Resilience Plan – NRRP, Mission 4, Component 2, Investment 1.3 – D.D. 1243 2/8/2022, PE0000005), and within the Space It Up project, funded by the Italian Space Agency, ASI and the Ministry of University and Research, MUR, under contract n. 2024-5-E.0 - CUP n. I53D24000060005. The work was supported by the "The Geosciences for Sustainable Development" project (Budget Ministero dell'Università e della Ricerca–Dipartimenti di Eccellenza 2023–2027 C93C23002690001). MA was supported by the Med World consortium, funded by the Council for Higher Education in Israel; and by the Israel Science Foundation research grant (ISF's No. 4089/25) and the Maimonides Fund's Future Scientists Center. We thank Marika Koukoula and Nadav Peleg for handling parts of the rain gauge data. We also gratefully acknowledge the WWLLN consortium for generously providing the lightning data.

Appendix A Data availability and statistical software

Information about the 792,786 precipitation storm time series extracted and analyzed in this study is provided in the form of an open dataset (Papacharalampous et al. 2026). This dataset includes the precipitation storm series, without timestamps or location information but labelled by storm type (as "type-1 major", "type-2 major", "moderate", "type-1 minor", or "type-2 minor"). A separate set of information provides the geographical location where each storm was observed indicated by its longitude and latitude, the timestamps at the storm initiation and termination, the storm features that drove the proposed typology on an algorithmic basis (i.e., maximum intensity, total volume, total duration, and coefficient of variation), and the storm type. The two sets of information use different storm identifiers; thus, they are not linkable. The labelled storm series can support, for example, analysis of storm-level characteristics of Alpine storms, validation of the typology using alternative clustering methods, or synthetic storm generation. The remaining information can support, for instance, spatially and temporally explicit analyses of Alpine storm characteristics, their drivers when combined with external time series or other additional data, and further validation of the typology using other datasets or independent event catalogues. The original time series cannot be shared by the authors. Their sources are the following:

- Agenzia Regionale per la Prevenzione e Protezione Ambientale del Veneto (https://www.arpa.veneto.it).
- Autorità di Bacino Distrettuale Fiume Po (https://www.adbpo.it).
- GeoSphere Austria (https://data.hub.geosphere.at/dataset/klima-v1-10min).
- Météo-France (https://meteo.data.gouv.fr).
- MeteoSwiss (https://www.meteoswiss.admin.ch).
- Provincia Autonoma di Bolzano (https://meteo.provincia.bz.it/default.asp).
- Provincia Autonoma di Trento (https://www.provincia.tn.it).

Data processing relied on a combination of the `R` (R Core Team 2024) and `MATLAB` programming languages. The statistical analyses and visualizations were conducted in `R`, with the exception of the computational analyses on spatial clustering, including the creation of Figure 4, which were performed in `MATLAB`. The following `R` packages were utilized: `bdc` (Ribeiro et al. 2024), `cluster` (Maechler et al. 2023), `data.table` (Barrett et al. 2024), `devtools` (Wickham et al. 2022), `dplyr` (Wickham et al. 2023a), `elevatr` (Hollister 2023), `ggpubr` (Kassambara 2023), `ggridges` (Wilke 2024), `gplots` (Warnes et al. 2024), `knitr` (Xie 2014, 2015, 2024), `lubridate` (Grolemund and Wickham 2011, Spinu et al. 2024), `raster` (Hijmans 2025), `RColorBrewer` (Neuwirth 2022), `readxl` (Wickham and Bryan 2023), `rmarkdown` (Allaire et al. 2024, Xie et al. 2018, 2020), `rnaturalearth` (Massicotte and South 2023), `scales` (Wickham et al. 2023b), `streamMetabolizer` (Appling et al. 2018) and `tidyverse` (Wickham et al. 2019, Wickham 2023). Equivalent codes to those used for this study for extracting the precipitation storm time series can be found in Marra (2024).

References

[1] Allaire JJ, Xie Y, Dervieux C, McPherson J, Luraschi J, Ushey K, Atkins A, Wickham H, Cheng J, Chang W, Iannone R (2024) rmarkdown: Dynamic Documents for R. R package version 2.29. https://CRAN.R-project.org/package=rmarkdown.

[2] Amponsah W, Marchi L, Zoccatelli D, Boni G, Cavalli M, Comiti F, Crema S, Lucía A, Marra F, Borga M (2016) Hydrometeorological characterisation of a flash flood associated with major geomorphic effects: Assessment of peak discharge uncertainties and analysis of the runoff response, Journal of Hydrometeorology 17:3063–3077. https://doi.org/10.1175/JHM-D-16-0081.1.

[3] Appling AP, Hall Jr RO, Yackulic CB, Arroita M (2018) Overcoming equifinality: Leveraging long time series for stream metabolism estimation. Journal of Geophysical Research: Biogeosciences 123(2):624–645. https://doi.org/10.1002/2017JG004140.

[4] Araujo DS, Marra F, Ali H, Fowler HJ, Nikolopoulos EI (2023) Relation between storm characteristics and extreme precipitation statistics over CONUS. Advances in Water Resources 178:104497. https://doi.org/10.1016/j.advwatres.2023.104497.

[5] Avanzi F, De Michele C, Gabriele S, Ghezzi A, Rosso R (2015) Orographic signature on extreme precipitation of short durations. Journal of Hydrometeorology 16:278–294. https://doi.org/10.1175/JHM-D-14-0063.1.

[6] Barrett T, Dowle M, Srinivasan A, Gorecki J, Chirico M, Hocking T, Schwendinger B (2024) data.table: Extension of 'data.frame'. R package version 1.16.4. https://CRAN.R-project.org/package=data.table.

[7] Beck HE, Zimmermann NE, McVicar TR, Vergopolan N, Berg A, Wood EF (2018) Present and future Köppen-Geiger climate classification maps at 1-km resolution. Scientific Data, 5(1):1–12. https://doi.org/10.1038/s41597-023-02549-6.

[8] Blanchet J, Reverdy A, Blanc A, Creutin JD, Kiennemann P, Evin G (2025) Linking torrential flood event occurrence to weather-type conditional driving atmospheric conditions—The case of the Northern French Alps. Journal of Hydrology: Regional Studies 59:102402. https://doi.org/10.1016/j.ejrh.2025.102402.

[9] Blöschl G, Bierkens MFP, Chambel A, Cudennec C, Destouni G, Fiori A, Kirchner JW, McDonnell JJ, Savenije HHG, Sivapalan M, et al. (2019) Twenty-three Unsolved Problems in Hydrology (UPH) – A community perspective. Hydrological Sciences Journal 64(1):1141–1158. https://doi.org/10.1080/02626667.2019.1620507.

[10] Borga M, Comiti F, Ruin I, Marra F (2019) Forensic analysis of flash flood response. Wiley Interdisciplinary Reviews: Water 6(2):e1338. https://doi.org/10.1002/wat2.1338.

[11] Borga M, Vezzani C, Dalla Fontana G (2005) Regional rainfall depth–duration–frequency equations for an alpine region. Natural Hazards 36(1):221–235. https://doi.org/10.1007/s11069-004-4550-y.

[12] Breugem AJ, Wesseling JG, Oostindie K, Ritsema CJ (2020) Meteorological aspects of heavy precipitation in relation to floods–an overview. Earth-Science Reviews 204:103171. https://doi.org/10.1016/j.earscirev.2020.103171.

[13] Buzzi A, Tartaglione N, Malguzzi P (1998) Numerical simulations of the 1994 Piedmont flood: Role of orography and moist processes. Monthly Weather Review 126(9):2369–2383. https://doi.org/10.1175/1520-0493(1998)126<2369:NSOTPF>2.0.CO;2.

[14] Cipolla G, Francipane A, Noto L (2020) Classification of extreme rainfall for a Mediterranean region by means of atmospheric circulation patterns and reanalysis data. Water Resources Management 34(10):3219–3235. https://doi.org/10.1007/s11269-020-02609-1.
[15] Correa-Sánchez N, Dallan E, Marra F, Fosser G, Borga M (2025) Orographic control on bias and uncertainty in extreme sub-daily precipitation simulations from a convection-permitting ensemble. Journal of Hydrology 659:133324. https://doi.org/10.1016/j.jhydrol.2025.133324.
[16] Dallan E, Borga M, Zaramella M, Marra F (2022) Enhanced summer convection explains observed trends in extreme subdaily precipitation in the Eastern Italian Alps. Geophysical Research Letters 49(5):e2021GL096727. https://doi.org/10.1029/2021GL096727.
[17] Dallan E, Marra F, Fosser G, Marani M, Formetta G, Schär C, Borga M (2023) How well does a convection-permitting regional climate model represent the reverse orographic effect of extreme hourly precipitation?. Hydrology and Earth System Sciences 27(5):1133–1149. https://doi.org/10.5194/hess-27-1133-2023.
[18] Dallan E, Borga M, Fosser G, Canale A, Roghani B, Marani M, Marra F (2024) A method to assess and explain changes in sub-daily precipitation return levels from convection-permitting simulations. Water Resources Research 60(5):e2023WR035969. https://doi.org/10.1029/2023WR035969.
[19] Dallan E, Marra F, Papacharalampous GA, Fowler H, Borga M (2025) Climatology of storm characteristics for sub-daily heavy precipitation in the Greater Alpine Region. ESS Open Archive. https://doi.org/10.22541/essoar.176487365.52815673/v1.
[20] Davolio S, Della Fera S, Laviola S, Miglietta MM, Levizzani V (2020) Heavy precipitation over Italy from the Mediterranean storm “Vaia” in October 2018: Assessing the role of an atmospheric river. Monthly Weather Review 148(9):3571–3588. https://doi.org/10.1175/MWR-D-20-0021.1.
[21] Destro E, Amponsah W, Nikolopoulos EI, Marchi L, Marra F, Zoccatelli D, Borga M (2018) Coupled prediction of flash flood response and debris flow occurrence: Application on an alpine extreme flood event. Journal of Hydrology 558:225–237. https://doi.org/10.1016/j.jhydrol.2018.01.021.
[22] D’Odorico P, Fagherazzi S, Rigon R (2005) Potential for landsliding: Dependence on hyetograph characteristics. Journal of Geophysical Research: Earth Surface 110(F1). https://doi.org/10.1029/2004JF000127.
[23] Estermann R, Rajczak J, Velasquez P, Lorenz R, Schär C (2025) Projections of heavy precipitation characteristics over the greater Alpine region using a kilometer–scale climate model ensemble. Journal of Geophysical Research: Atmospheres 130(2):e2024JD040901. https://doi.org/10.1029/2024JD040901.
[24] Feloni EG, Baltas EA, Nastos PT, Matsangouras IT (2019) Implementation and evaluation of a convective/stratiform precipitation scheme in Attica region, Greece. Atmospheric Research 220:109–119. https://doi.org/10.1016/j.atmosres.2019.01.011.
[25] Fischer S, Schumann AH (2024) Temporal changes in the frequency of flood types and their impact on flood statistics. Journal of Hydrology X 22:100171. https://doi.org/10.1016/j.hydroa.2024.100171.
[26] Fischer S, Schumann AH (2021) Regionalisation of flood frequencies based on flood type-specific mixture distributions. Journal of Hydrology X 13:100107. https://doi.org/10.1016/j.hydroa.2021.100107.

[27] Fischer S, Schumann A, Bühler P (2019) Timescale-based flood typing to estimate temporal changes in flood frequencies. Hydrological Sciences Journal 64(15):1867–1892. https://doi.org/10.1080/02626667.2019.1679376.
[28] Flaounas E, Aragão L, Bernini L, Dafis S, Doiteau B, Flocas H, Gray SL, Karwat A, Kouroutzoglou J, Lionello P, et al. (2023) A composite approach to produce reference datasets for extratropical cyclone tracks: Application to Mediterranean cyclones, Weather and Climate Dynamics 4:639–661. https://doi.org/10.5194/wcd-4-639-2023.
[29] International Journal of Climatology: A Journal of the Royal Meteorological Society 18(8):873–900. https://doi.org/10.1002/(SICI)1097-0088(19980630)18:8%3C873::AID-JOC255%3E3.0.CO;2-9.
[30] Grazzini F, Craig GC, Keil C, Antolini G, Pavan V (2020) Extreme precipitation events over northern Italy. Part I: A systematic classification with machine-learning techniques. Quarterly Journal of the Royal Meteorological Society 146(726):69–85. https://doi.org/10.1002/qj.3635.
[31] Grolemund G, Wickham H (2011) Dates and times made easy with lubridate. Journal of Statistical Software 40(3):1–25. https://doi.org/10.18637/jss.v040.i03.
[32] Gustafsson N, Janjić T, Schraff C, Leuenberger D, Weissmann M, Reich H, Brousseau P, Montmerle T, Wattrelot E, Bučánek A, et al. (2018) Survey of data assimilation methods for convective-scale numerical weather prediction at operational centres. Quarterly Journal of the Royal Meteorological Society 144(713):218–1256. https://doi.org/10.1002/qj.3179.
[33] Hastie T, Tibshirani R, Friedman J (2009) The Elements of Statistical Learning: Data Mining, Inference and Prediction, second edition. Springer, New York. https://doi.org/10.1007/978-0-387-84858-7.
[34] Herrera RV, Blenkinsop S, Guerreiro SB, Fowler HJ (2023) The creation and climatology of a large independent rainfall event database for Great Britain. International Journal of Climatology 43(13):6020–6037. https://doi.org/10.1002/joc.8187.
[35] Hirschboeck KK (1988) Flood Hydroclimatology. In: Baker VR, Kochel RC, Patton PC (Eds) Flood Geomorphology. Wiley-Interscience.
[36] Hijmans R (2025) raster: Geographic Data Analysis and Modeling. R package version 3.6-31. https://CRAN.R-project.org/package=raster.
[37] Hollister JW (2023) elevatr: Access Elevation Data from Various APIs. R package version 0.99.0. https://CRAN.R-project.org/package=elevatr.
[38] Hopke PK, Kaufman L (1990) The use of sampling to cluster large data sets. Chemometrics and Intelligent Laboratory Systems 8(2):195–204. https://doi.org/10.1016/0169-7439(90)80135-S.
[39] Isotta FA, Frei C, Weilguni V, Percec Tadic M, Lassegues P, Rudolf B, Pavan V, Cacciamani C, Antolini G, Ratto SM, et al. (2014) The climate of daily precipitation in the Alps: Development and analysis of a high-resolution grid dataset from pan-Alpine rain-gauge data. International Journal of Climatology 34(5):1657–1675. https://doi.org/10.1002/joc.3794.
[40] James G, Witten D, Hastie T, Tibshirani R (2013) An Introduction to Statistical Learning. Springer, New York. https://doi.org/10.1007/978-1-4614-7138-7.
[41] Kaczmarska J, Isham V, Onof C (2014) Point process models for fine-resolution rainfall. Hydrological Sciences Journal 59(11):1972–1991. https://doi.org/10.1080/02626667.2014.925558.

[42] Kahraman A, Kendon EJ, Chan SC, Fowler HJ (2021) Quasi-stationary intense rainstorms spread across Europe under climate change. Geophysical Research Letters 48(13):e2020GL092361. https://doi.org/10.1029/2020GL092361.

[43] Kahraman A, Kendon EJ, Fowler HJ, Wilkinson JM (2022) Contrasting future lightning stories across Europe. Environmental Research Letters 17(11):114023. https://doi.org/10.1088/1748-9326/ac9b78.

[44] Kassambara A (2023) ggpubr: 'ggplot2' Based Publication Ready Plots. R package version 0.6.0. https://CRAN.R-project.org/package=ggpubr.

[45] Kaufman L, Rousseeuw PJ (1990) Finding Groups in Data: An Introduction to Cluster Analysis. Wiley, New York.

[46] Kendall MG (1975) Rank Correlation Methods, fourth edition. Charles Griffin, London.

[47] Laaha G, Laimighofer J, Özcelik NB, Fischer S (2025) Exploring process heterogeneity in environmental statistics: Examples and methodological advances. Austrian Journal of Statistics 54(3):124–149. https://doi.org/10.17713/ajs.v54i3.2101.

[48] Llasat MC, del Moral A, Cortès M, Rigo T (2021) Convective precipitation trends in the Spanish Mediterranean region. Atmospheric Research 257:105581. https://doi.org/10.1016/j.atmosres.2021.105581.

[49] Maechler M, Rousseeuw P, Struyf A, Hubert M, Hornik K (2023) cluster: Cluster Analysis Basics and Extensions. R package version 2.1.6. https://CRAN.R-project.org/package=cluster.

[50] Mann HB (1945) Non-parametric tests against trend. Econometrica 13:163–171. https://doi.org/10.2307/1907187.

[51] Maraun D, Shepherd TG, Widmann M, Zappa G, Walton D, Gutiérrez JM, Hagemann S, Richter I, Soares PMM, Hall A, Mearns LO (2017) Towards process-informed bias correction of climate change simulations. Nature Climate Change 7(11):764–773. https://doi.org/10.1038/nclimate3418.

[52] Markonis Y, Kumar R, Hanel M, Rakovec O, Máca P, AghaKouchak A (2021) The rise of compound warm-season droughts in Europe. Science Advances 7(6):eabb9668. https://doi.org/10.1126/sciadv.abb9668.

[53] Marra F (2024) A unified framework for extreme sub-daily precipitation frequency analyses based on ordinary events - data & codes. (Version v1.2) [Software]. Zenodo. https://doi.org/10.5281/zenodo.11934843.

[54] Marra F, Nikolopoulos EI, Creutin JD, Borga M (2014) Radar rainfall estimation for the identification of debris-flow occurrence thresholds. Journal of Hydrology 519(Part B):1607–1619. https://doi.org/10.1016/j.jhydrol.2014.09.039.

[55] Marra F, Borga M, Morin E (2020) A unified framework for extreme subdaily precipitation frequency analyses based on ordinary events. Geophysical Research Letters 47(18):e2020GL090209. https://doi.org/10.1029/2020GL090209.

[56] Marra F, Armon M, Adam O, Zoccatelli D, Gazal O, Garfinkel CI, Rostkier-Edelstein D, Dayan U, Enzel Y, Morin E (2021) Toward narrowing uncertainty in future projections of local extreme precipitation. Geophysical Research Letters 48(5):e2020GL091823. https://doi.org/10.1029/2020GL091823.

[57] Marra F, Koukoula M, Canale A, Peleg N (2024) Predicting extreme sub-hourly precipitation intensification based on temperature shifts. Hydrology and Earth System Sciences 28(2):375–389. https://doi.org/10.5194/hess-28-375-2024.

[58] Marra F, Dallan E, Canale A, Prosdocimi I, Papacharalampous GA, Borga M, Papalexiou SM (2026) Apparent heavy tails of sub-daily precipitation explained by the coexistence of lighter-tailed processes. Geophysical Research Letters 53(2):e2025GL119705. https://doi.org/10.1029/2025GL119705.
[59] Massicotte P, South A (2023) rnaturalearth: World Map Data from Natural Earth. R package version 1.0.1. https://CRAN.R-project.org/package=rnaturalearth.
[60] Ménégoz M, Valla E, Jourdain NC, Blanchet J, Beaumet J, Wilhelm B, Gallée H, Fettweis X, Morin S, Anquetin S (2020) Contrasting seasonal changes in total and intense precipitation in the European Alps from 1903 to 2010. Hydrology and Earth System Sciences 24(11):5355–5377. https://doi.org/10.5194/hess-24-5355-2020.
[61] Merz B, Aerts J, Arnbjerg-Nielsen K, Baldi M, Becker A, Bichet A, Blöschl G, Bouwer LM, Brauer A, Cioffi F, et al. (2014) Floods and climate: Emerging perspectives for flood risk assessment and management. Natural Hazards and Earth System Sciences 14:1921–1942. https://doi.org/10.5194/nhess-14-1921-2014.
[62] Merz R, Blöschl G (2003) A process typology of regional floods. Water Resources Research 39(12). https://doi.org/10.1029/2002WR001952.
[63] Napoli A, Parodi A, von Hardenberg J, Pasquero C (2023) Altitudinal dependence of projected changes in occurrence of extreme events in the Great Alpine Region. International Journal of Climatology 43(12):5813–5829. https://doi.org/10.1002/joc.8222.
[64] Neuwirth E (2022) RColorBrewer: ColorBrewer Palettes. R package version 1.1-3. https://CRAN.R-project.org/package=RColorBrewer.
[65] Oppel H, Fischer S (2020) A new unsupervised learning method to assess clusters of temporal distribution of rainfall and their coherence with flood types. Water Resources Research 56(5):e2019WR026511. https://doi.org/10.1029/2019WR026511.
[66] Papacharalampous GA, Dallan E, Armon M, Saha J, Price C, Borga M, Marra F (2026) Precipitation-driven typology of storms in the Alps: Data (Version v2) [Dataset]. Zenodo. https://doi.org/10.5281/zenodo.19264262.
[67] Papadopoulos A, Chronis TG, Anagnostou EN (2005) Improving convective precipitation forecasting through assimilation of regional lightning measurements in a mesoscale model. Monthly Weather Review 133(7):1961–1977. https://doi.org/10.1175/MWR2957.1.
[68] Peleg N, Morin E (2014) Stochastic convective rain-field simulation using a high-resolution synoptically conditioned weather generator (HiReS-WG). Water Resources Research 50(3):2124–2139. https://doi.org/10.1002/2013WR014836.
[69] Peleg N, Koukoula M, Marra F (2025) A 2C warming can double the frequency of extreme summer downpours in the Alps. npj Climate and Atmospheric Science 8:216. https://doi.org/10.1038/s41612-025-01081-1.
[70] Pineda N, Tomeu R, Joan B, Xavier S (2007) Lightning and precipitation relationship in summer thunderstorms: Case studies in the North Western Mediterranean region. Atmospheric Research 85(2):159–170. https://doi.org/10.1016/j.atmosres.2006.12.004.
[71] R Core Team (2024) R: A language and environment for statistical computing. R Foundation for Statistical Computing, Vienna, Austria. https://www.r-project.org.

[72] Ribeiro B, Velazco S, Guidoni-Martins K, Tessarolo G, Jardim L (2024) bdc: Biodiversity Data Cleaning. R package version 1.1.5. https://CRAN.R-project.org/package=bdc.
[73] Rodger CJ, Werner S, Brundell JB, Lay EH, Thomson NR, Holzworth RH, Dowden RL (2006) Detection efficiency of the VLF world-wide lightning location network (WWLLN): Initial case study. Annales Geophysical 24(12):3197–3214. https://doi.org/10.5194/angeo-24-3197-2006.
[74] Rubel F, Brugger K, Haslinger K, Auer I (2017) The climate of the European Alps: Shift of very high resolution Köppen-Geiger climate zones 1800–2100. Meteorologische Zeitschrift 26(2):115-125. https://doi.org/10.1127/metz/2016/0816.
[75] Ruiz-Leo AM, Hernández E, Queralt S, Maqueda G (2013) Convective and stratiform precipitation trends in the Spanish Mediterranean coast. Atmospheric Research 119:46–55. https://doi.org/10.1016/j.atmosres.2011.07.019.
[76] Rulfová Z, Kyselý J (2013) Disaggregating convective and stratiform precipitation from station weather data. Atmospheric Research 134:100–115. https://doi.org/10.1016/j.atmosres.2013.07.015.
[77] Rulfová Z, Kyselý J (2014) Trends of convective and stratiform precipitation in the Czech Republic, 1982–2010. Advances in Meteorology 2014:647938. https://doi.org/10.1155/2014/647938.
[78] Soriano LR, De Pablo F, Díez EG (2001) Relationship between convective precipitation and cloud-to-ground lightning in the Iberian Peninsula. Monthly Weather Review 129(12):2998–3003. https://doi.org/10.1175/1520-0493(2001)129<2998:RBCPAC>2.0.CO;2.
[79] Sottile G, Francipane A, Adelfio G, Noto LV (2022) A PCA-based clustering algorithm for the identification of stratiform and convective precipitation at the event scale: An application to the sub-hourly precipitation of Sicily, Italy. Stochastic Environmental Research and Risk Assessment 36(8):2303–2317. https://doi.org/10.1007/s00477-021-02028-7.
[80] Spinu V, Grolemund G, Wickham H (2024) lubridate: Make Dealing with Dates a Little Easier. R package version 1.9.4. https://CRAN.R-project.org/package=lubridate.
[81] Stein L, Pianosi F, Woods R (2020) Event-based classification for global study of river flood generating processes. Hydrological Processes 34(7):1514–1529. https://doi.org/10.1002/hyp.13678.
[82] Tarasova L, Merz R, Kiss A, Basso S, Blöschl G, Merz B, Viglione A, Plötner S, Guse B, Schumann A, et al. (2019) Causative classification of river flood events. Wiley Interdisciplinary Reviews: Water 6(4):e1353. https://doi.org/10.1002/wat2.1353.
[83] Tarasova L, Basso S, Wendi D, Viglione A, Kumar R, Merz R (2020) A process-based framework to characterize and classify runoff events: The event typology of Germany. Water Resources Research 56(5):e2019WR026951. https://doi.org/10.1029/2019WR026951.
[84] Tremblay A (2005) The stratiform and convective components of surface precipitation. Journal of the Atmospheric Sciences 62(5):1513–1528. https://doi.org/10.1175/JAS3411.1.

[85] Treppiedi D, Cipolla G, Noto LV (2023) Convective precipitation over a Mediterranean area: From identification to trend analysis starting from high-resolution rain gauges data. International Journal of Climatology 43(1):293–313. https://doi.org/10.1002/joc.7758.
[86] Tseng CY, Wang LP, Onof C (2025) Modelling convective cell life cycles with a copula-based approach. Hydrology and Earth System Sciences 29(1):1–25. https://doi.org/10.5194/hess-29-1-2025.
[87] Turkington T, Breinl K, Ettema J, Alkema D, Jetten V (2016) A new flood type classification method for use in climate change impact studies. Weather and Climate Extremes 14:1–16. https://doi.org/10.1016/j.wace.2016.10.001.
[88] Virts KS, Wallace JM, Hutchins ML, Holzworth RH (2013) Highlights of a new ground-based, hourly global lightning climatology. Bulletin of the American Meteorological Society 94(9):1381–1391. https://doi.org/10.1175/bams-d-12-00082.1.
[89] Warnes G, Bolker B, Bonebakker L, Gentleman R, Huber W, Liaw A, Lumley T, Maechler M, Magnusson A, Moeller S, et al. (2024) gplots: Various R Programming Tools for Plotting Data. R package version 3.2.0. https://CRAN.R-project.org/package=gplots.
[90] Weisse AK, Bois P (2001) Topographic effects on statistical characteristics of heavy rainfall and mapping in the French Alps. Journal of Applied Meteorology 40(4):720–740. https://doi.org/10.1175/1520-0450(2001)040<0720:TEOSCO>2.0.CO;2.
[91] Wickham H (2023) tidyverse: Easily Install and Load the 'Tidyverse'. R package version 2.0.0. https://CRAN.R-project.org/package=tidyverse.
[92] Wickham H, Averick M, Bryan J, Chang W, McGowan LD, François R, Grolemund G, Hayes A, Henry L, Hester J, et al. (2019) Welcome to the tidyverse. Journal of Open Source Software 4(43):1686. https://doi.org/10.21105/joss.01686.
[93] Wickham H, Bryan J (2023) readxl: Read Excel Files. R package version 1.4.3. https://CRAN.R-project.org/package=readxl.
[94] Wickham H, Hester J, Chang W, Bryan J (2022) devtools: Tools to Make Developing R Packages Easier. R package version 2.4.5. https://CRAN.R-project.org/package=devtools.
[95] Wickham H, François R, Henry L, Müller K, Vaughan D (2023a) dplyr: A Grammar of Data Manipulation. R package version 1.1.4. https://CRAN.R-project.org/package=dplyr.
[96] Wickham H, Pedersen T, Seidel D (2023b) scales: Scale Functions for Visualization. R package version 1.3.0. https://CRAN.R-project.org/package=scales.
[97] Wilke C (2024) ggridges: Ridgeline Plots in 'ggplot2'. R package version 0.5.6. https://CRAN.R-project.org/package=ggridges.
[98] Xie Y (2014) knitr: A Comprehensive Tool for Reproducible Research in R. In: Stodden V, Leisch F, Peng RD (Eds) Implementing Reproducible Computational Research. Chapman and Hall/CRC.
[99] Xie Y (2015) Dynamic Documents with R and knitr, second edition. Chapman and Hall/CRC.
[100] Xie Y (2024) knitr: A General-Purpose Package for Dynamic Report Generation in R. R package version 1.49. https://CRAN.R-project.org/package=knitr.
[101] Xie Y, Allaire JJ, Grolemund G (2018) R Markdown: The Definitive Guide. Chapman and Hall/CRC. ISBN 9781138359338. https://bookdown.org/yihui/rmarkdown.

[102] Xie Y, Dervieux C, Riederer E (2020) R Markdown Cookbook. Chapman and Hall/CRC. ISBN 9780367563837. https://bookdown.org/yihui/rmarkdown-cookbook.
[103] Zhou K, Zheng Y, Li B, Dong W, Zhang X (2019) Forecasting different types of convective weather: A deep learning approach. Journal of Meteorological Research 33:797–809. https://doi.org/10.1007/s13351-019-8162-6.